REPORT DOCUMENTATION PAGE

AFRL-SR-AR-TR-05-

0366

1. AGENCY USE ONLY *(Leave blank)*	2. REPORT DATE	3. REP~
		01 May 2004 - 30 Apr 2005 FINAL

4. TITLE AND SUBTITLE
Generation and Study of Microwave Plasma Jets

5. FUNDING NUMBERS
61102F
2301/EX

6. AUTHOR(S)
Dr Kuo

7. PERFORMING ORGANIZATION NAME(S) AND ADDRESS(ES)
POLYTECHNIC UNIVERSITY
SIX METROTECH CENTER
BROOKLYN NY 11201-2915

8. PERFORMING ORGANIZATION REPORT NUMBER

9. SPONSORING/MONITORING AGENCY NAME(S) AND ADDRESS(ES)
AFOSR/NE
4015 WILSON BLVD
SUITE 713
ARLINGTON VA 22203

10. SPONSORING/MONITORING AGENCY REPORT NUMBER
FA9550-~~~~~~-04-1-0352

11. SUPPLEMENTARY NOTES

12a. DISTRIBUTION AVAILABILITY STATEMENT
DISTRIBUTION STATEMENT A: Unlimited

12b. DISTRIBUTION CODE

13. ABSTRACT *(Maximum 200 words)*

The present report summarizes the work, under the support of the AFOSR Grant AFOSR-FA9550-04-1-0352, starting at May 1, 2004.

This research program is primarily aiming at developing plasma torches as igniters of a scramjet engine. For the hydrocarbon-fueled scramjet in a typical startup scenario, cold liquid JP-7 is injected into a Mach-2 air crossflow (having a static temperature of $-\sim$ 500 K); under these conditions, the fuel-air mixture will not auto-ignite. Some ignition aid, for example, plasma torches that can deliver enough heat to the mixture to reduce the ignition delay time and to increase the rate of combustion, is necessary to initiate main-duct combustion.

A cylindrical torch module improved from the previous one (United States Patent No.: US 6329628 B1) has been designed. It was fabricated at AFRL, Hanscom and tested at Polytechnic University. The central electrode is made of a tungsten tube, rather than a tungsten rod, adding an additional flow path through the tungsten tube that can be used for fuel injection purpose. The gas plenum chamber is integrated to the module. Moreover, we have developed a unique way to couple microwave to the arc plasma generated by this new torch module. We integrate the torch module into a tapered rectangular cavity.

14. SUBJECT TERMS

15. NUMBER OF PAGES

16. PRICE CODE

17. SECURITY CLASSIFICATION OF REPORT	18. SECURITY CLASSIFICATION OF THIS PAGE	19. SECURITY CLASSIFICATION OF ABSTRACT	20. LIMITATION OF ABSTRACT
Unclassified	Unclassified	Unclassified	UL

Annual Technical Report on Air Force Office of Scientific

Research Grant AFOSR-FA9550-04-1-0352

Generation and Study of Microwave Plasma Jets

Spencer P. Kuo, Principal Investigator

Daniel Bivolaru, Research Scientist

Department of Electrical & Computer Engineering

Polytechnic University

6 Metrotech Center

Brooklyn, NY 11201

I.   Introduction

The present report summarizes the work, under the support of the AFOSR Grant AFOSR-FA9550-04-1-0352, starting at May 1, 2004.

This research program is primarily aiming at developing plasma torches as igniters of a scramjet engine. For the hydrocarbon-fueled scramjet in a typical startup scenario, cold liquid JP-7 is injected into a Mach-2 air crossflow (having a static temperature of ~ 500 K); under these conditions, the fuel-air mixture will not auto-ignite. Some ignition aid, for example, plasma torches that can deliver enough heat to the mixture to reduce the ignition delay time and to increase the rate of combustion, is necessary to initiate main-duct combustion.

A cylindrical torch module improved from the previous one (United States Patent No.: US 6329628 B1) has been designed. It was fabricated at AFRL, Hanscom and tested at Polytechnic University. The central electrode is made of a tungsten tube, rather than a tungsten rod, adding an additional flow path through the tungsten tube that can be used for fuel injection purpose. The gas plenum chamber is integrated to the module. Moreover, we have developed a unique way to couple microwave to the arc plasma generated by this new torch module. We integrate the torch module into a tapered rectangular cavity as shown in Fig. 1.
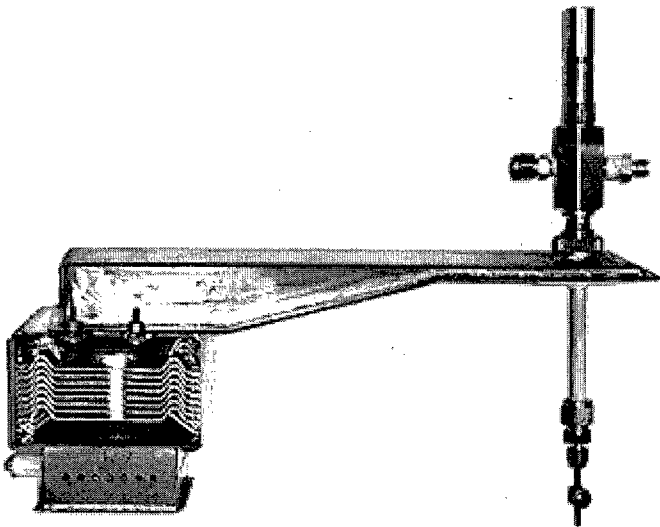

Fig.1 A photo of the microwave-augmented plasma torch module.

Thus microwave energy in this adaptor arrangement can easily be delivered from the cavity to the arc plasma without hindering the access of the torch module to the combustor cavity or adding any significant complexity to the design. In order to be effective as an igniter, the torch plasma has to penetrate deeply into the supersonic cross flow in the combustor. The arc torch relies on the applied gas flow to push the torch plasma, which has to overcome the momentum of the supersonic crossflow. The microwave-augmented torch plasma can penetrate deeply into the supersonic crossflow even when the torch is operated at relatively low gas flow rate. This is because the microwave field is not affected by the supersonic crossflow in the combustor. Consequently, the temperature and average energy of the microwave-augmented torch plasma is significantly higher than that of the arc torch plasma, which has to operate at a much higher gas flow rate to achieve a similar penetration depth into the supersonic cross flow.

II. DESCRIPTION OF THE DEVICE

The components of this plasma torch device include 1) a 2.45 GHz, 1.5 kW magnetron as the microwave source, 2) a tapered microwave cavity, 3) a torch module, and 4) a power supply to run the torch module and the magnetron. This torch module is similar to that developed by Kuo *et al* (1999, 2001, 2004a), with the exceptions that the device is longer and has an integrated gas plenum chamber allowing for the module to be integrated into a supersonic combustor. Moreover, the central electrode has been replaced with a tungsten carbide tube providing an additional flow path for either air or fuel. The remaining components consist of a high power transformer, diodes, and capacitors. The transformer uses a single-phase input from 208 V power line and has a 1:17 turn ratio. This power supply initiates the arc discharge on the first cycle after power is applied to the transformer. However, a few seconds are required to heat-up the filament of the magnetron before the torch operates in a microwave-augmented mode.

An S-band rectangular waveguide having a cross section of 7.2 cm × 3.4 cm is tapered to a cross section of 7.2 cm × 0.5 cm. The two ends of the waveguide are terminated by conducting plates to form a rectangular cavity. This cavity consists of three

sections. Two sections with uniform cross section are connected by a tapered section. The first section (cross section of 7.2 cm × 3.4 cm) has a length of $3\lambda_z/8$ and the last section (cross section of 7.2 cm × 0.5 cm) has a length of $\lambda_z/2$ where $\lambda_z = \lambda_0/[1 - (\lambda_0/2\alpha)^2]^{1/2} = 23.3$ cm is the axial wavelength for the TE_{103} mode, $\lambda_0 = 12.25$ cm is the free space wavelength, and $\alpha = 7.2$ cm is the dimension of the wider side of the cross section. The middle transition section, tapering the cross section from 7.2 cm × 3.4 cm to 7.2 cm × 0.5 cm, has a length of $\lambda_z/2$ and a slope angle $\theta = 14^0$. This cavity is similar to the one used in a microwave torch device reported previously (Kuo $et\ al$ 2004b).

Microwave generated by a magnetron (2.45 GHz, 700 W to 1.5 kW) radiates into this cavity at a location about quarter wavelength $(\lambda_0/4)$ (more precisely, $\lambda_z/8$) away from the shorted-end of the non-tapered section of the cavity. The quarter wavelength in the axial direction of the uniform sections of the cavity is 5.83 cm and the wavelength in the middle transition section is expected to be a little shorter; thus, the total axial length of 32 cm matches the length requirement for the TE_{103} cavity mode. This result is confirmed by the measurements described later.

In the narrow section of the cavity, two aligned holes on the bottom and top walls of the cavity at a distance $\lambda_z/8 = 2.92$ cm away from the end are introduced. The top hole has a diameter of 9.53 mm and a tube fitting is welded to it. A torch module is then installed through the holder, as shown in the photo of Fig. 1, by inserting the bottom part containing only the central electrode and the ceramic insulator of the torch module through these two aligned holes. The bottom hole on the cavity wall has the same diameter of 9.53 mm fitted exactly to the ceramic insulator. The portion of the central electrode of the torch module inside the cavity functions as a receiving antenna and the portion (~ 143 mm) of the torch module above the top wall of the cavity functions as an open-end transmission line. In this configuration, the plasma torch module becomes a microwave adaptor. In Fig. 1, a magnetron with its transmitting antenna inserted into the cavity from the other side (non-tapered section) is also shown. When plasma is generated by the arc discharge between the electrodes of the torch module, the plasma produces a time varying resistive load of the adaptor. The effectiveness of delivering microwave through this adaptor to a dynamic load will be analyzed and presented in the next section.

The cylindrical torch module, which uses the frame of a cylindrical tube having an outer diameter of 16.5 mm as the grounded outer electrode, is described here. The concentric electrodes in the module are separated at the nozzle exit location by a gap of 2.16 mm and insulated by a ceramic tube, having outer and inner diameters of 9.53 mm and 3.81 mm, respectively, and dielectric constant $\varepsilon_r = 8$, which hosts the central electrode. The frame, having a length of 143 mm, consists of three sections. The bottom section is 51 mm in length, having an inner diameter slightly larger than 9.53 mm to accommodate the ceramic insulator. The central section has a length of 90 mm and has a much large inner diameter of 12.7 mm so that this section functions as a gas plenum chamber. A threaded nozzle of 2 mm length is inserted at the top of the frame to increase the gas flow speed in the discharge region. This nozzle has an inner diameter of 7.5 mm. The ceramic insulator does not cover the central electrode in the nozzle. It is placed slightly below the bottom of the nozzle. The central electrode is a tungsten carbide tube with inner and outer diameters of 1.14 mm and 3.18 mm, respectively, and fits tightly inside the ceramic insulator. The hollow center section can be connected to a separate gas supply allowing for an additional, independent flow path through the discharge region. The flow path through the center of the tungsten carbide tube is used for injection of ethylene fuel in the present study. However, any gas can be used in either the inner or outer flow paths.

Both the torch module and magnetron operate at the power line frequency, typically 60 Hz, with approximately a 50% duty cycle. Hence, the synchronization of the two components in each cycle is essential to the operation of this hybrid torch module. The optimal operation condition is when the arc discharge pulse of the torch module and the microwave pulse of the magnetron overlap in time. The microwave field is too small to initiate discharge by itself for the microwave power used in the present setup. Since the discharge pulse is shorter than the microwave pulse, the arc discharge needs to start at the beginning of the steady-state level of the microwave pulse. Thus, the two components share the same power supply to simplify the synchronization.

Fig. 2 shows a circuit diagram of the power supply used in this study, which is capable of operating the arc discharge and the magnetron simultaneously. A single power transformer with a turn ratio of 1:17 is used to step up the 60-Hz line voltage of 208 V
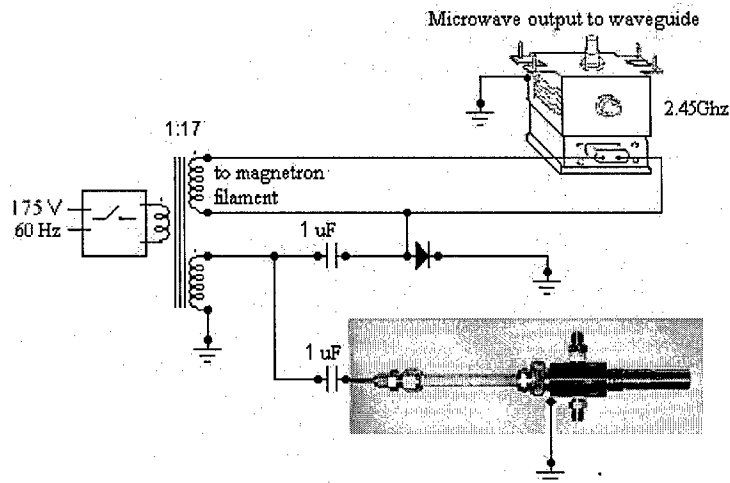
FIG. 2 Schematic circuit diagram of the combined power supply.

(rms) to 3.5 kV (rms), which is applied to both devices through two (one for each device) serially connected $1\mu F/2.3$ kVAC capacitors. However, since neither device requires the full 3.5 kV (rms) in their operations, a Variac is used to reduce the input voltage from 208 V to 175 V. The magnetron, which has a grounded anode, is then connected in parallel with a diode (15 kV and 750 mA rating) to assure that only negative voltages are applied to the cathode. The arc discharge occurs in both the positive and negative voltage cycles of the AC input; the plasma generated during negative-voltage discharges directly interacts with the magnetron output pulses, and the plasma generated during the positive-voltage discharges interacts with remaining microwave energy stored in the cavity.

The arc discharge draws too much current from the power supply for the capacitor in the magnetron circuit to maintain the required voltage for turning on the magnetron. Consequently, the magnetron is automatically turned off during the peak of arc discharge. Although the magnetron operation is interrupted by the arc discharge, the arc discharge still provides seed charges to interact with the main pulse of the microwave, which extends the duration of the plasma pulse. After the arc discharge, the voltage returns to a high value, and the output power of the "restarted" magnetron increases considerably. The coupling of the two loads improves the power factor of the power line from 0.52 to 0.89.

III. COUPLING EFFICIENCY

The torch module has a coaxial structure and can easily be connected to a rectangular waveguide to form a microwave adaptor. A schematic of such an arrangement is shown in Fig. 3a. In this adaptor, the antenna size is equal to b, the dimension of the short side of the waveguide, because the central electrode of the module has to pass through the waveguide to be accessible to high voltage connection for the arc discharge. This size is different from that of the conventional adaptor, which is usually less than b/2. Two serially connected transmission lines shown in Fig. 3b are used to represent the torch module, i.e., the detail of the short nozzle section of the torch module, which is much shorter than the wavelength, is not included in the analysis. The central electrode is tightly fit to the ceramic insulator so that no air gap exists between the two components.
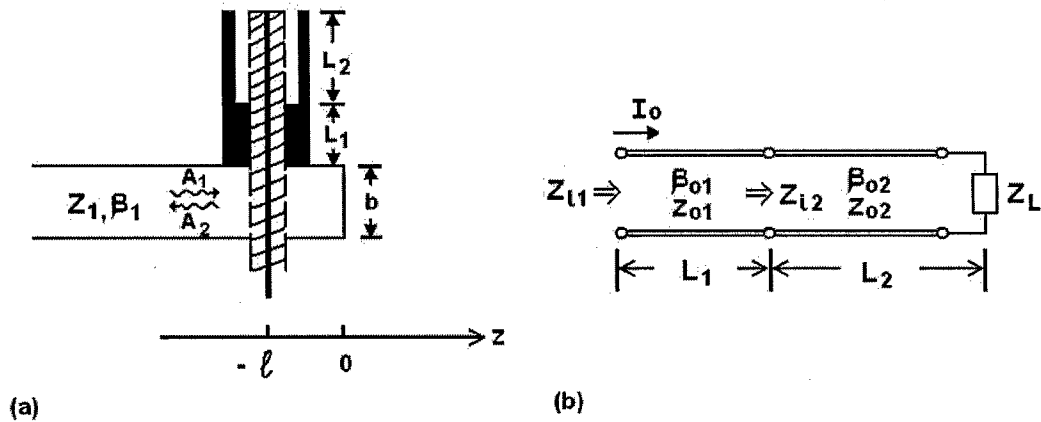

FIG. 3   (a) Schematic of the microwave adaptor and (b) equivalent transmission line model of the torch module.

The characteristic impedances Z_0 and propagation constants β_0 of these two transmission lines are determined to be

$$Z_{01} = (60/\sqrt{\varepsilon_r})\ln(r_{01}/r_i) \ \Omega$$

$$Z_{02} = 60\{\ln(r_{02}/r_i)[\varepsilon_r^{-1}\ln(r_{01}/r_i) + \ln(r_{02}/r_{01})]\}^{1/2} \ \Omega \qquad (1)$$

$$\beta_{01} = k_0\sqrt{\varepsilon_r}$$

$$\beta_{02} = k_0\{\ln(r_{02}/r_i)/[\varepsilon_r^{-1}\ln(r_{01}/r_i) + \ln(r_{02}/r_{01})]\}^{1/2}$$

7

where $k_0 = \omega_0/c$ is the wave number in free space, ω_0 is the wave angular frequency, c is the speed of light in free space, r_i and r_{01} are the outer radii of the central electrode and the ceramic insulator, respectively, and r_{02} is the inner radius of the gas plenum chamber (central section of the torch frame).

When the arc discharge is initiated, the plasma becomes a time varying resistive load, represented by R_L, of the combined line. The antenna inside the waveguide receives the microwave power to make a current source as the input of the line. The microwave power coupling efficiency depends on the matching condition of the load. However, the plasma is a dynamic load, i.e., time varying resistive load, so perfect impedance matching over the operational range is not possible. In the following, an analysis to determine the dependence of the coupling efficiency on R_L is presented.

The input impedances of line 1 and line 2 are Z_{i1} and Z_{i2} as shown in Fig. 3b. Introducing the normalized impedances $\mathfrak{z}_{i1} = Z_{i1}/Z_{01}$, $\mathfrak{z}_{i2} = Z_{i2}/Z_{02}$, and $\mathfrak{z}_\ell = Z_L/Z_{02}$, and the notations $a_1 = \tan\beta_{01}L_1$, $a_2 = \tan\beta_{02}L_2$, and $\eta = Z_{02}/Z_{01}$, allows the input impedances to be expressed as

$$\mathfrak{z}_{i1} = (\eta\mathfrak{z}_{i2} + ja_1)/(1 + j\eta\mathfrak{z}_{i2}a_1) \tag{2}$$

and

$$\mathfrak{z}_{i2} = (\mathfrak{z}_\ell + ja_2)/(1 + j\,\mathfrak{z}_\ell\, a_2). \tag{3}$$

Substituting Equation (3) into Equation (2), the following expression is obtained for the input impedance

$$\mathfrak{z}_{i1} = [\mathfrak{z}_\ell\,(\eta - a_1a_2) + j(\eta a_2 + a_1)]/[(1 - \eta a_1a_2) + j\,\mathfrak{z}_\ell\,(\eta a_1 + a_2)] = \mathcal{R}_{i1} + j\chi_{i1}. \tag{4}$$

The input impedance $\mathfrak{z}_{i1}$ of the combined line given by Equation (4) represents the load impedance of the antenna which is expressed as a function of the actual load impedance $\mathfrak{z}_\ell$ of the system. Considering only TE_{10} mode in the waveguide of Fig. 3a, the phasors of the wave fields are given by

$$\mathbf{E} = \hat{\mathbf{y}} \begin{cases} \sin(\pi x/a)[A_1\exp(-j\beta_1 z) + A_2\exp(j\beta_1 z)] & \text{for } z < -\ell \\ \\ B\sin(\pi x/a)\sin(\beta_1 z) & \text{for } -\ell < z < 0 \end{cases} \tag{5}$$

$$H = \hat{x} \begin{cases} -Z_1^{-1}\sin(\pi x/a)[A_1\exp(-j\beta_1 z) - A_2\exp(j\beta_1 z)] & \text{for } z < -\ell \\ \\ -jZ_1^{-1}B \sin(\pi x/a) \cos(\beta_1 z) & \text{for } -\ell < z < 0 \end{cases} \quad (6)$$

where $Z_1 = \omega_0\mu_0/\beta_1 = \eta_0 k_0/\beta_1$ is the wave impedance in the waveguide; μ_0 is the free space permeability, $\eta_0 = 377 \ \Omega$ is the intrinsic impedance of the free space, and $\beta_1 = 2\pi/\lambda_z$ is the wave propagation constant in the waveguide; $A_2 = \Gamma A_1$, here $\Gamma = \Gamma_r + j\Gamma_i$ is the reflection coefficient. $\Gamma = 0$ only when the load is matched to the line and the reflectance $|\Gamma|^2$ determines the coupling efficiency (given by $1- |\Gamma|^2$). The continuity condition of the wave electric field at $z = - \ell$ leads to $A_1\exp(j\beta_1\ell) + A_2\exp(-j\beta_1\ell) = - B \sin(\beta_1\ell)$, which reduces to $B = -(\sin\beta_1\ell)^{-1}[1 + \Gamma\exp(-2j\beta_1\ell)] A_1\exp(j\beta_1\ell)$.

This wave electric field induces an antenna current density given by

$$\mathbf{J} = \hat{y} \ I_0\sin(\pi y/2b)\delta(x - a/2)\delta(z + \ell) \quad \text{for } 0 \leq y \leq b \quad (7)$$

where $y = 0$ and $y = b$ are located on the bottom and top plates of the waveguide shown in Fig. 3a, respectively. At $y = b$, the antenna current is $I = I_0$, which is the input current of the combined transmission line shown in Fig. 3b. The net time average microwave power received by the antenna is given by

$$P_0 = -\tfrac{1}{2}\!\int \mathbf{E} \times \mathbf{H}^* \cdot d\mathbf{S} = \tfrac{1}{2}\!\int \mathbf{E} \cdot \mathbf{J}^* \, dV. \quad (8)$$

This power should equal to the net input power of the transmission line, which is given by $\tfrac{1}{2} |I_0|^2 Z_{i1}$. Thus the power balance condition leads to the following equations

$$-\tfrac{1}{2}\!\int \mathbf{E} \times \mathbf{H}^* \cdot d\mathbf{S} = \tfrac{1}{2}\!\int \mathbf{E} \cdot \mathbf{J}^* \, dV = \tfrac{1}{2} |I_0|^2 Z_{i1.} \quad (9)$$

Substituting Equations (4) – (7) into Equation (9), results in two coupled real equations for Γ_r and Γ_i being obtained. The coefficients of the equations are functions of the variable parameter ℓ and the location of the antenna (torch module). Those coefficients are simplified by considering two preferential locations: $\ell = \lambda_z/8$ and $\lambda_z/4$, i.e., $\beta_1\ell = \pi/4$ and $\pi/2$.

Case A. $\ell = \lambda_z/8$. The coupled equations are given by

$$(1 - \Gamma_r^2 - \Gamma_i^2)/(1 + \Gamma_r^2 + \Gamma_i^2 + 2\Gamma_r + 2\Gamma_i) = -\mathscr{R}_{i1}/\chi_{i1} \quad (10)$$

and

$$(1 + \Gamma_r + \Gamma_i)[(1+\Gamma_i)^2+\Gamma_r^2]/[(1 - \Gamma_r^2 - \Gamma_i^2)^2 + (1 + \Gamma_r^2 + \Gamma_i^2 + 2\Gamma_r + 2\Gamma_i)^2]$$

$$= (\pi^2 a Z_{01}/16 b Z_1)(\mathcal{R}_{i1} - \chi_{i1}) \qquad (11)$$

where $\mathcal{R}_{i1}$ and χ_{i1}, given by Equation (4), are functions of the load impedance $\mathfrak{z}_\ell$.

Case B. $\ell = \lambda_z/4$. **The coupled equations become**

$$(1 - \Gamma_r^2 - \Gamma_i^2)/2\Gamma_i = -\mathcal{R}_{i1}/\chi_{i1} \qquad (12)$$

$$[(1 - \Gamma_r)^2 + \Gamma_i^2]^2/[(1 - \Gamma_r^2 - \Gamma_i^2)^2 + 4\Gamma_i^2] = (\pi^2 a Z_{01}/8 b Z_1)^2 \, | \mathfrak{z}_{i1}|^2. \qquad (13)$$

These two sets of two equations [(10) and (11), and (12) and (13)] will be solved to obtain $|\Gamma|^2(\mathfrak{z}_\ell)$ for comparison.

Using the dimensions of the torch device presented in this work yields $Z_{01} = 24.5$ Ω, $Z_{02} = 47.4$ Ω, $Z_1 = 682$ Ω, $\beta_{01} = 2.83$ k_0, $\beta_{02} = 1.83$ k_0, and $\beta_1 = 1.81$ k_0, where $k_0 = 16.67\pi$, $a = 72$ mm and $b = 5$ mm. Thus $a_1 = 2.1$, $a_2 = -0.72$, and $\eta = 1.93$, which reduces Equation (4) to $\mathfrak{z}_{i1} = [1.03 \, \mathfrak{z}_\ell + j(0.18 - 0.75 \, \mathfrak{z}_\ell^2)]/(1 + 0.72 \, \mathfrak{z}_\ell^2) = \mathcal{R}_{i1} + j\chi_{i1}$. With the aide of these parametric values, Equation sets (10) & (11) and (12) & (13) are solved numerically. The results $|\Gamma_A|^2(\mathfrak{z}_\ell)$ and $|\Gamma_B|^2(\mathfrak{z}_\ell)$ are presented in Figs. 4a and b, respectively. As shown in the figures, $|\Gamma_A|^2 < |\Gamma_B|^2$; moreover, $|\Gamma_A|^2 < 0.2$ for $38 \, \Omega < Z_L < 200 \, \Omega$, while $|\Gamma_B|^2 > 0.2$ in the same region. This impedance region corresponds to the times before and after the peak of the arc discharge. In the setup, the magnetron and the arc torch module share the same power supply to eliminate the need of an additional circuit to synchronize the microwave pulse with the arc discharge. Hence, the magnetron operation is affected by the arc discharge, which causes voltage to drop considerably. As shown in the preceding section, the magnetron is off during the peak of the arc discharge due to the voltage drop during the arc discharge. In other words, during the high reflectance time period when torch plasma has very low impedance, the voltage drop automatically shuts off the magnetron. This automatic shutoff feature also improves the coupling efficiency of this microwave adaptor. The results presented in the next section are obtained by using Case A arrangement with $\ell = \lambda_z/8$.
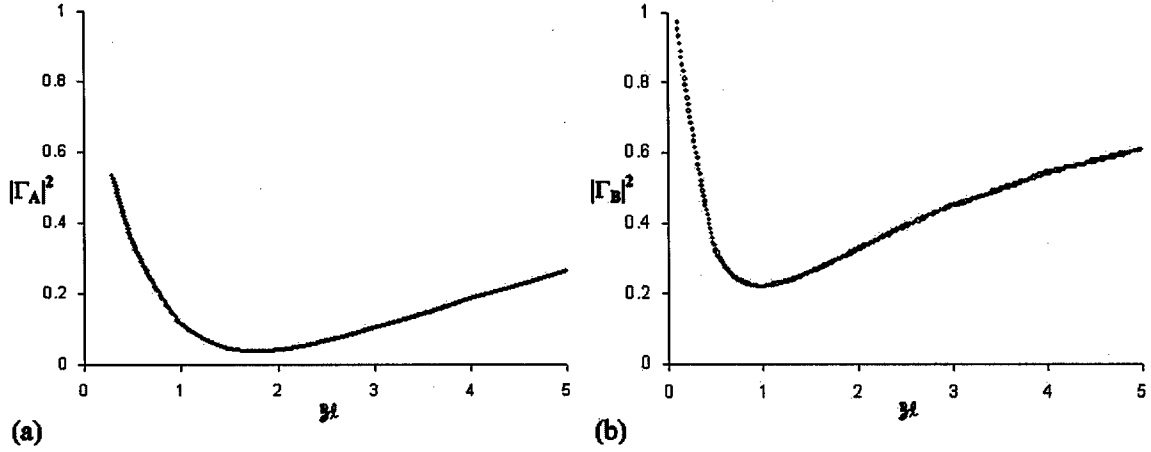
FIG. 4 Reflectance $|\Gamma|^2$ of the adaptor as a function of the load resistance $\mathcal{R}$ for two different torch module locations: (a) $\ell = \lambda_z/8$ and (b) $\lambda_z/4$ from the endplate.

IV. MICROWAVE EFFECT ON TORCH PLASMA

The torch is operated in the open air using compressed air as the feedstock. The torch module operates stably over a very large flow rate range, with flow speeds from subsonic to supersonic. The effect of microwave power on the torch plasma varies with the gas flow rate. This dependence is demonstrated by the single frame CCD plasma plume images shown in Fig. 5. The five sets of images with microwave off (top row) and on (bottom row) from (a) to (e) correspond to the air supply pressures of 1.36, 2.04, 3.4, 4.76, and 5.44 atm absolute, respectively, where the flow speeds at the nozzle exit of the torch module are subsonic in (a) to (c) and are supersonic in (d) and (e). As shown in the figure, the applied microwave power can increase the height and the volume of the torch plasma significantly at low gas flow rates. Comparing the top- and bottom-row plume images in (a) to (e), it is seen that, with the application of microwave power, the respective plume heights increase by more than 300%, 100%, 30%, 20%, and 10%, and the respective plume volumes increase by approximately 900%, 400%, 180%, 100%, and 50%. The enhancement is estimated from the increased luminosity of the plasma plume which provides an indirect measurement. The effect of applying the microwave power decreases with increasing flow speed. As the air supply pressure is increased, thereby
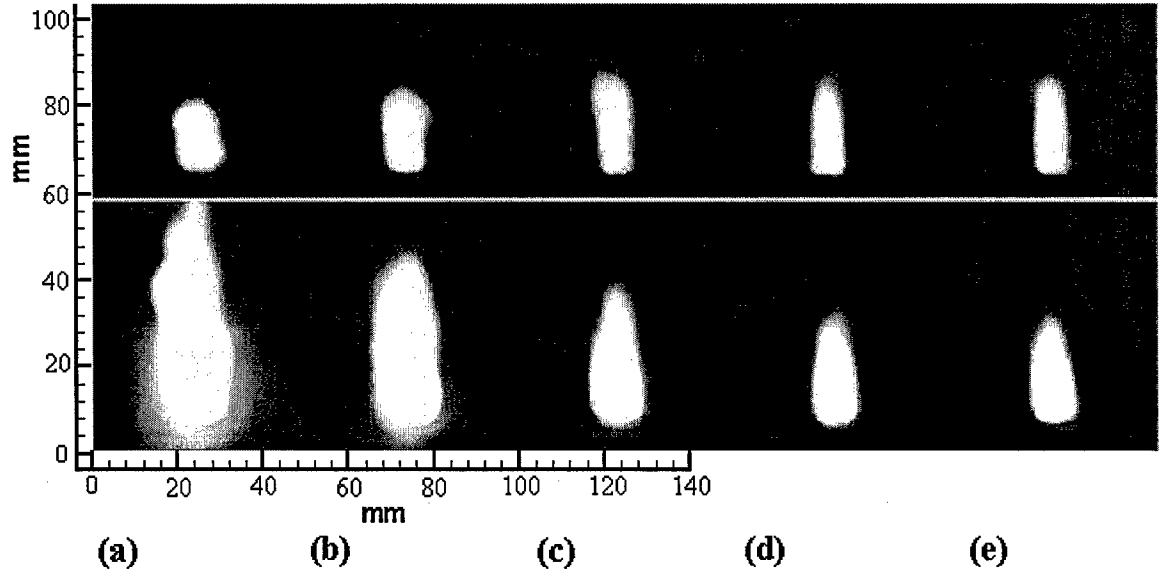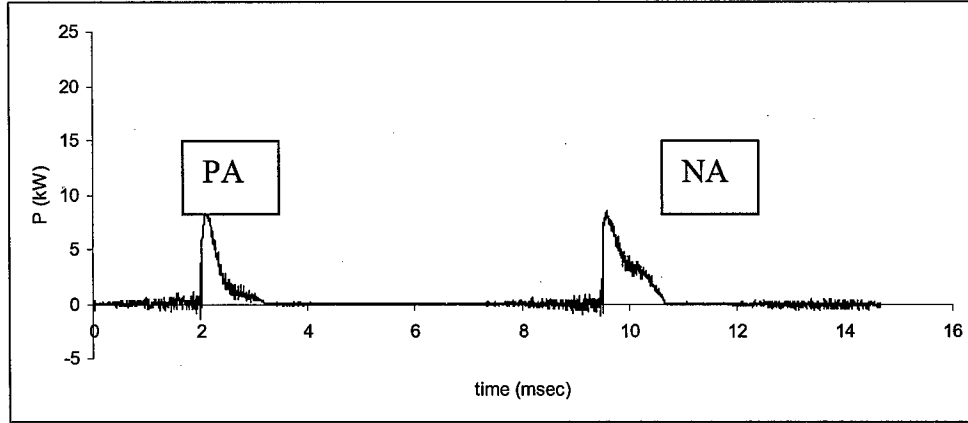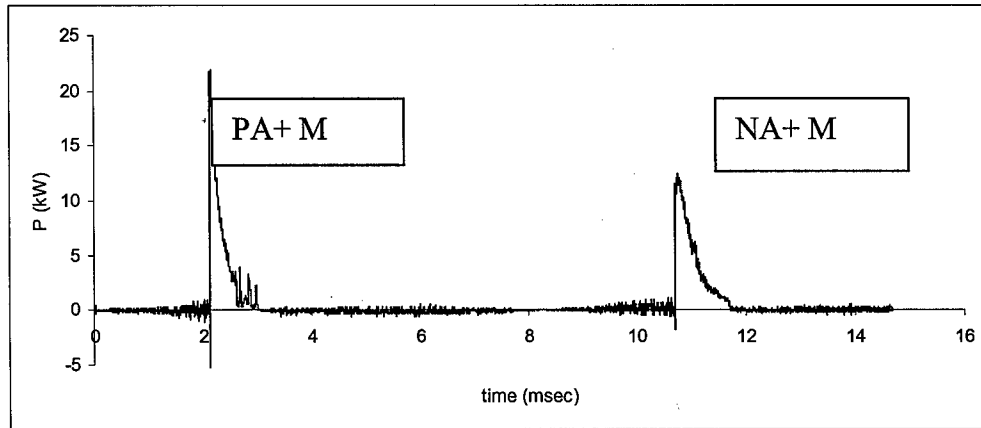
11

FIG. 5 Images of plasma plumes generated before (top row) and after (bottom row) the magnetron is turned on. The air supply pressures in (a) to (e) are 1.36, 2.04, 3.4, 4.76, and 5.44 atm.

increasing the flow speed, the size of the arc torch plasma shown in the top row of Fig. 5 also increases except at the transition from subsonic (c) to supersonic (d). Alternatively, the plume sizes of the microwave-enhanced torch plasmas shown in the bottom row of Fig. 5 decrease with increasing flow speed but are still enhanced compared the arc only images as indicated by lower luminosity of the arc only plasma plumes. This dependence most likely results from the fact that the fixed applied power has to energize more gas with less interaction time as the flow rate increases, and the size of the torch plasma becomes dictated by the flow speed. At the same supply pressure, the heights of the microwave-augmented torch plasmas shown in (d) and (e) are only slightly larger than the corresponding arc torch plasmas. However, the volume and the luminosity intensity of the plasma plume are still increased by the application of the microwave power.

The time varying voltage V and current I of the discharge were measured using a digital oscilloscope. The product of the V and I functions gives the instantaneous power function. The arc discharge occurs in each half cycle, but magnetron runs only during the negative-voltage half cycle. Thus the microwave pulse lasting approximately 6 ms is expected to synchronize only with the negative discharge pulse. However, the arc discharge affects the operation of the magnetron. In fact, the magnetron is shut off during

12

(a)

Chart (a): P (kW) vs time (msec). Y-axis: 25, 20, 15, 10, 5, 0, -5. X-axis: 0, 2, 4, 6, 8, 10, 12, 14, 16. Labeled boxes: PA, NA.

(b)

Chart (b): P (kW) vs time (msec). Y-axis: 25, 20, 15, 10, 5, 0, -5. X-axis: 0, 2, 4, 6, 8, 10, 12, 14, 16. Labeled boxes: PA+ M, NA+ M.

FIG. 6 The power of the 60 Hz arc discharge. (a), the positive arc (PA) and negative arc (NA); (b), microwave field applied to the positive arc (PA+M), and negative arc (NA+M).

the main pulse of the arc discharge. It turns out that the microwave effect on the positive discharge is stronger than that on the negative discharge in the case of low flow rate. The power functions in one cycle for discharges without and with the presence of microwave in the case of low flow rate are presented in Figs. 6a and b for comparison. The supply pressure of the torch module is 1.16 atm. The powers plotted in Fig. 6 are calculated from the current drawn by the arc discharge and the voltage drop across the two electrodes, i.e., no contribution from the magnetron is included. As shown, the microwave has enhanced both the peak power of the negative discharge and the positive discharge. The peak power in the negative discharge pulse is increased from 8 kW to 12 kW. However, the total energy per pulse does not increase proportionally, because the discharge pulse energy is limited by the available energy stored in the capacitors, which does not change

significantly. In the arc discharge, the voltage and current peaks are not in phase. The voltage reaches the peak of about 4 kV when the gaseous breakdown starts. As the discharge current increases, the discharge voltage drops rapidly to a relatively low level in the range of 200 to 400 V. Thus, at the peak current the discharge voltage is in fact quite low, which limits the peak discharge power. The microwave helps to reduce the phase delay of the current peak from the voltage peak resulting in a higher discharge voltage while the discharge current is increasing. The V-I characteristic plots shown in Figs. 7a and b, for discharges without and with the presence of microwave, respectively, also demonstrate this point. As shown the peaks of the arc discharge currents in both cases are about the same. However, the areas of the hysteresis loops in Fig. 7b are larger than the corresponding ones in Fig. 7a, and the arc discharge voltages at large current values (Fig. 7b) are higher. Consequently, the peak of the product of the V and I functions is increased. It is also indicated in Fig. 7b that microwave increases considerably the breakdown voltage in the positive discharge. When the central electrode is positive, it collects electrons produced by the discharge. The microwave field enhances the electron mobility, and thus the transit-time loss of electrons to the central electrode, which in turn increases the breakdown voltage. The microwave effect on the positive discharge is likely attributed to the circuit arrangement and cavity setup. The negative arc discharge delays the start of the magnetron and the cavity prolongs the storing time of the remaining microwave after the negative arc discharge.

(a)   (b
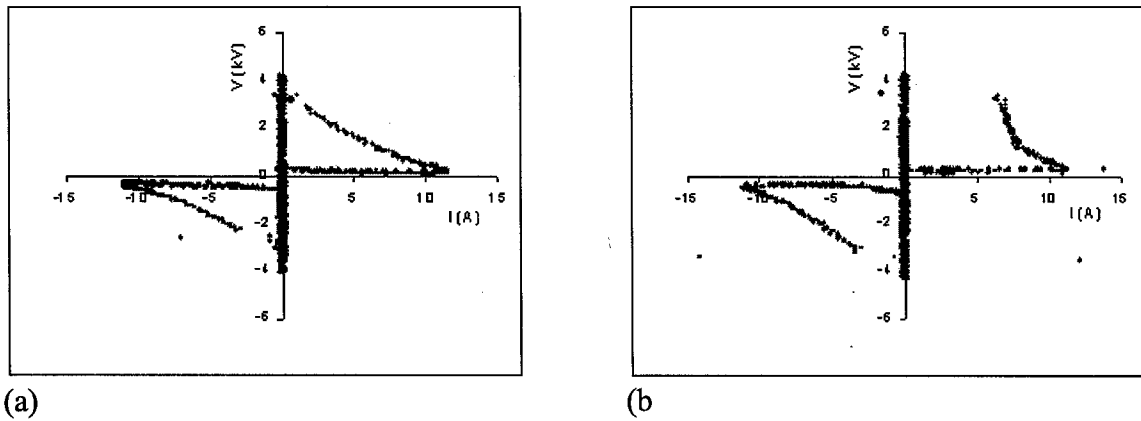
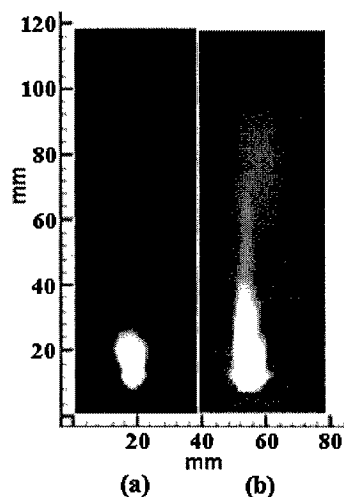FIG. 7   V-I   characteristics   of   discharges   (a)   without   microwave   and   (b)   with   microwave.

FIG. 9 Torch plasmas plumes, (a) air plasma generated by arc discharges and (b) flame plume (in the center) ignited by 60-Hz microwave torch plasma; in both cases gaseous ethylene fuel (flow rate of 20 SLM) was injected through the central electrode (tungsten-carbide tube), and an airflow rate of 30 SLM was supplied.

Experiments demonstrating the torch module as a fuel injector and igniter of hydrocarbon fuel have also been performed. Tests have been conducted using gaseous ethylene fuel with the flow rate of 9 standard liters per minute (SLM) injected through the central electrode, a tungsten-carbide tube, corresponding to 160 m/s fuel velocity at 298 K. The flame plume was observed when the torch was run with air flow rates ranging from 10-100 SLM with microwave power applied. This air flow rate range corresponded to air velocities of 6-65 m/s at 298 K. Ignition under these conditions is illustrated in Fig. 8b. The plasma plume of the arc discharge (without microwave) operated in the same condition is shown in Fig. 8a for comparison. As shown, fuel was not ignited. This effect is understood because fuel was injected from the central port of the module, which was outside the main arc discharge region. An estimate of the discharge region can be seen in the images shown in Fig. 9.
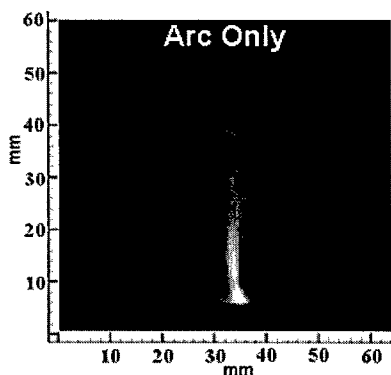
(a)
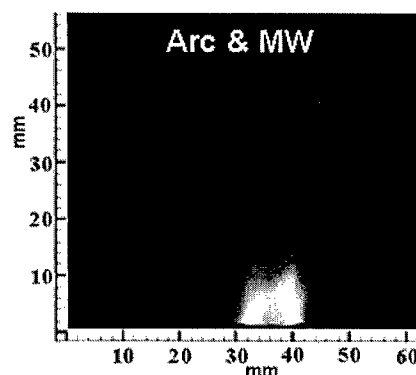
(b)

FIG. 9 Plasma plume emission images recorded with an interline-transfer CCD camera image with an 100 μs exposure; the illuminated portions shown correspond to the discharge region generated by (a) an arc discharge and (b) an arc discharge in the presence of the microwave.

15

Fig. 9a is the arc plasma plume emission image recorded with an interline-transfer CCD camera with a 100 μs exposure. This image was recorded though a 1 nm bandpass interference filter centered at 405 nm, and the high intensity region was correlated to energy deposition by the plasma. However, as microwave was introduced, the torch plasma distributes more uniformly across the electrodes as seen in Fig. 9b. In Fig. 9b, the plasma distribution is more uniform and has a higher density in the central region of the hollow central electrode where the fuel is ejected. The microwave energy has also significantly enhanced the size and enthalpy (evidenced by the luminosity) of the torch plasma. It is noted that the arc discharge alone can also ignite the fuel as the discharge power is increased by increasing the capacitance in the power supply from 1 μF to 3 μF. Under these conditions, a maximum of 400 SLM air flow rate was ignited while maintaining the ethylene flow rate at 9 SLM.

V. SUMMARY AND CONCLUSIONS

A torch device that integrates a cylindrical-shaped plasma torch module into a tapered rectangular microwave cavity is developed. The central electrode of the torch module is inserted through the tapered side of the cavity at $\lambda_z/8$ distance away from the end wall to function as a receiving antenna; and the microwave power injected into the cavity from the other end is delivered to the torch plasma generated by the torch module through this coupling. In the presence of seed charges provided by the arc discharge, the required microwave field intensity for the initiating the microwave discharge is well below the microwave breakdown threshold field. Thus, the present microwave-augmented torch module employs a power level low enough to avoid undesired microwave breakdown inside the cavity but high enough to introduce significant microwave enhancement of the arc discharge.

A theoretical analysis on the microwave coupling efficiency shows that nearly 80% of the supplied microwave power can be delivered to the arc plasma through this adaptor arrangement. Experiments performed demonstrate that the added microwave energy increases the height and the volume of torch plasma considerably. The magnitude of the microwave enhancement decreases as the air flow rate increases. Nevertheless, the height and the volume of microwave-augmented torch plasma exceed those of the arc

16

torch plasma even when the flow speed is supersonic. The added microwave power also affects the peak power delivered by the arc discharge by affecting the phase relationship of the current and voltage. The addition of the magnetron to the circuit increases the circuit efficiency enabling more power to be delivered to the gas.

The three principal advantages of the microwave-augmented device invented are: 1) It is compact and durable, running for long periods of time in a periodic mode on an air feedstock; 2) It needs very low gas flow rate in its operation, which is an essential requirement of a practical igniter; 3) It is able to run as a combined igniter/fuel injector. The microwave-augmented arc discharge operating with low gas flow rate delivers more energy to the gas over a larger volume, as evidenced by the measured powers and luminosity of the plasma plume, compared previous arc discharge configurations. This improvement should both prove beneficial for applications involving ignition and combustion in a variety of environments.

VI.   PUBLICATIONS

1.   S. P. Kuo and Steven S. Kuo, "A Physical Mechanism of Non-thermal Plasma Effect on Shock Wave", Phys. Plasmas, 12, 012315(1-5), Jan. 2005.

2.   Daniel Bivolaru and S. P. Kuo, "Aerodynamic Modification of supersonic flow around truncated cone using Pulsed Electrical Discharges", AIAA Journal, 43(7), 1482-1489, 2005.

3.   S. P. Kuo, "Shock Wave Modification by a Plasma Spike: Experiment and Theory", Physica Scripta, 71, 5, 535-539, 2005.

4.   Wilson Lai, Henry Lai, Spencer P. Kuo, Olga Tarasenko, and Kalle Levon, "Decontamination of Biological Warfare Agents by a Microwave Plasma Torch", Phys. Plasmas, 12, 023501 (1-6), Feb. 2005.

5.   S. P. Kuo, Daniel Bivolaru, Skip Williams, and Campbell D. Carter, "A Microwave-Augmented Plasma Torch Module", submitted to the Plasma Sources Science and Technology.